

How do Decisions Emerge across Layers in Neural Models? Interpretation with Differentiable Masking

Nicola De Cao

University of Edinburgh
University of Amsterdam
nicola.decao@uva.nl

Wilker Aziz

University of Amsterdam
w.aziz@uva.nl

Michael Schlichtkrull

University of Edinburgh
University of Amsterdam
m.s.schlichtkrull@uva.nl

Ivan Titov

University of Edinburgh
University of Amsterdam
ititov@inf.ed.ac.uk

Abstract

Attribution methods assess the contribution of inputs (e.g., words) to the model prediction. One way to do so is *erasure*: a subset of inputs is considered irrelevant if it can be removed without affecting the model prediction. Despite its conceptual simplicity, erasure is not commonly used in practice. First, the objective is generally intractable, and approximate search or leave-one-out estimates are typically used instead; both approximations may be inaccurate and remain very expensive with modern deep (e.g., BERT-based) NLP models. Second, the method is susceptible to the *hindsight bias*: the fact that a token can be dropped does not mean that the model ‘knows’ it can be dropped. The resulting pruning is over-aggressive and does not reflect how the model arrives at the prediction. To deal with these two challenges, we introduce Differentiable Masking. DIFFMASK relies on learning sparse stochastic gates (i.e., masks) to completely mask-out subsets of the input while maintaining end-to-end differentiability. The decision to include or disregard an input token is made with a simple linear model based on intermediate hidden layers of the analyzed model. First, this makes the approach efficient at test time because we predict rather than search. Second, as with probing classifiers, this reveals what the network ‘knows’ at the corresponding layers. This lets us not only plot attribution heatmaps but also analyze how decisions are formed across network layers. We use DIFFMASK to study BERT models on sentiment classification and question answering.

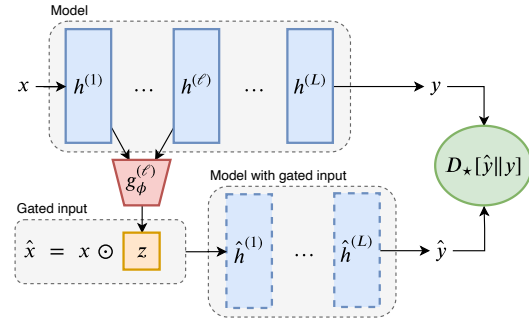


Figure 1: DIFFMASK: We take hidden states up to layer ℓ from a model (top) and feed them to a classifier g that predicts a mask z . We use this to mask the input and re-compute the forward pass (bottom). The classifier g is trained to mask as much of the input as possible without changing the output (minimizing a divergence D_*).

improvements over traditional approaches on many tasks (Goldberg, 2017). Their success is due to their ability to capture complex non-linear relations and induce powerful features. Unfortunately, their power and flexibility come at the expense of interpretability. This lack of interpretability can prevent users from trusting model predictions (Kim, 2015; Ribeiro et al., 2016), makes it hard to detect model or data deficiencies (Gururangan et al., 2018; Kaushik and Lipton, 2018) or verify that a model is fair and does not exhibit harmful biases (Sun et al., 2019; Holstein et al., 2019).

These challenges have motivated a massive amount of work on interpretability, both in NLP and generally in machine learning; see Belinkov and Glass (2019) and Jacovi and Goldberg (2020) for reviews. In this work, we study *post hoc interpretability* where the goal is to explain the prediction of a trained model and to reveal how the model arrives at the decision. This goal is usually approached with attribution methods (Bach et al.,

1 Introduction

Deep neural networks (DNN) have become standard tools in NLP demonstrating impressive im-

Code at: github.com/nicola-decao/DiffMask. Correspondence to Nicola De Cao nicola.decao@uva.nl.

Question: Where did the Broncos practice for the Super Bowl ?

Passage: The Panthers used the San Jose State practice facility and stayed at the San Jose Marriott . The Broncos practiced at Stanford University and stayed at the Santa Clara Marriott .

(a) Integrated Gradient (Sundararajan et al., 2017).

Question: Where did the Broncos practice for the Super Bowl ?

Passage: The Panthers used the San Jose State practice facility and stayed at the San Jose Marriott . The Broncos practiced at Stanford University and stayed at the Santa Clara Marriott .

(c) NLP explainer (Guan et al., 2019).

Question: Where did the Broncos practice for the Super Bowl ?

Passage: The Panthers used the San Jose State practice facility and stayed at the San Jose Marriott . The Broncos practiced at Stanford University and stayed at the Santa Clara Marriott .

(e) Erasure exact search optima.

Question: Where did the Broncos practice for the Super Bowl ?

Passage: The Panthers used the San Jose State practice facility and stayed at the San Jose Marriott . The Broncos practiced at Stanford University and stayed at the Santa Clara Marriott .

(b) Restricting the Flow (Schulz et al., 2020)

Question: Where did the Broncos practice for the Super Bowl ?

Passage: The Panthers used the San Jose State practice facility and stayed at the San Jose Marriott . The Broncos practiced at Stanford University and stayed at the Santa Clara Marriott .

(d) Our DIFFMASK.

Question: Where did the Broncos practice for the Super Bowl ?

Passage: The Panthers used the San Jose State practice facility and stayed at the San Jose Marriott . The Broncos practiced at Stanford University and stayed at the Santa Clara Marriott .

(f) Our DIFFMASK non-amortized.

Figure 2: Question Answering: Predictions of previous perturbation-based methods, (b) and (c), are misleading as they attribute the prediction mostly to the answer span itself (underlined). Our method (d) reveals that the model pays attention to the question type (e.g., the *where* token) as well as named entities and predicate ‘practice’. Predictions of the path-based methods (a) are more spread-out. Exact search leads to pathological attributions (e) and the same happens for our tractable but approximate search (f) when no amortization is used.

2015; Shrikumar et al., 2017; Sundararajan et al., 2017), which explain the behavior of a model by assigning relevance to inputs.

One way to perform attribution is to use *erasure* where a subset of features (i.e. usually input tokens) is considered irrelevant if it can be removed without affecting the model prediction (Li et al., 2016; Feng et al., 2018). The advantage of erasure is that it is conceptually simple and optimizes a well-defined objective. This contrasts with most other attribution methods which rely on heuristic rules to define feature salience, for example, attention-based attribution (Rocktäschel et al., 2015; Serrano and Smith, 2019; Vashishth et al., 2019) or back-propagation methods (Bach et al., 2015; Shrikumar et al., 2017; Sundararajan et al., 2017). These approaches received much scrutiny in recent years (Nie et al., 2018; Sixt et al., 2019; Jain and Wallace, 2019), as they cannot guarantee that the network is ignoring the low-scored features. They are often motivated as approximations of erasure (Baehrens et al., 2010; Simonyan et al., 2013; Feng et al., 2018) and sometimes even evaluated using erasure (e.g., Serrano and Smith (2019); Jain and Wallace (2019)).

Despite its conceptual simplicity, subset erasure is not commonly used in practice. First, it is generally **intractable**, and beam search (Feng et al., 2018) or leave-one-out estimates (Zintgraf et al., 2017) are typically used instead. These approximations may be inaccurate. For example, leave-one-out can underestimate contribution of features due to saturation (Shrikumar et al., 2017). More impor-

tantly, even these approximations remain very expensive with modern deep (e.g., BERT-based) models, as they require multiple computation passes through the model. Second, the method is **susceptible to the hindsight bias**: the fact that a feature *can be* dropped does not mean that the model ‘knows’ that it can be dropped and that the feature *is not* used by the model when processing the example. This results in over-aggressive pruning that does not reflect what information the model uses to arrive at the decision. The issue is pronounced in NLP tasks (see Figure 2e and Feng et al. (2018)), though it is easier to see on the following artificial example (Figure 3a). A model is asked to predict if there are more 7s than 1s in the sequence. The erasure attributes the prediction to a single 7 digit, as this reduced example yields the same decision as the original one. However, this does not reveal what the model was actually relying on: in fact it has counted digits 7 and 1 as otherwise it would not have achieved the perfect score on the test set.

We propose a new method, Differentiable Masking (DIFFMASK), which overcomes the aforementioned limitations and results in attributions that are more informative and help us understand how the model arrives at the prediction. DIFFMASK relies on learning sparse stochastic gates (i.e. masks), guaranteeing that the information from the masked-out inputs does not get propagated while maintaining end-to-end differentiability without having to resort to REINFORCE (Williams, 1992; Li et al., 2016). The decision to include or disregard an input

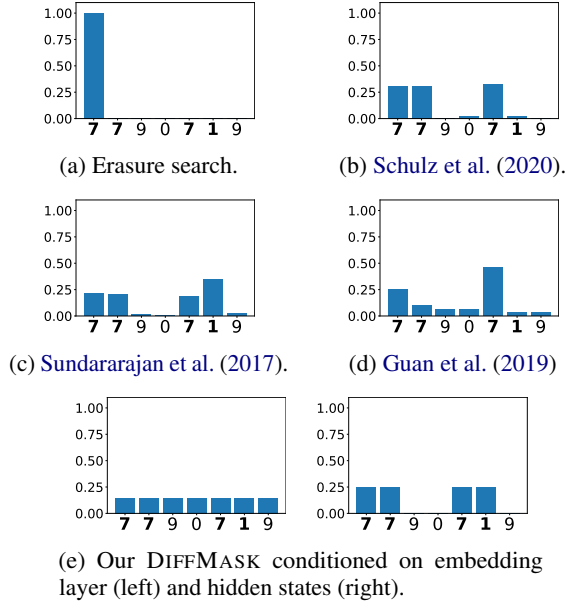


Figure 3: Input attributions of several methods on a toy task: Given a sequence x of digits and a query $\langle n, m \rangle$ (7 and 1 in this example) of two digits, determine whether there are more n than m in x . The query and input embeddings are concatenated, fed to a feed-forward NN, and then to a single layered GRU. Attributions are normalized to 1, for visualization.

token is made with a simple linear model based on intermediate hidden layers of the analyzed model (see Figure 1). First, this *amortization* circumvents the need for combinatorial search making the approach efficient at test time. Second, as with probing classifiers (Adi et al., 2017; Belinkov and Glass, 2019), this reveals whether the network ‘knows’ at the corresponding layer what input tokens can be masked.

The amortization lets us not only plot attribution heatmaps, as in Figure 2d, but also analyze how decisions are formed across network layers. In our artificial example, we can see that in the bottom embedding layer the model cannot discard any tokens, as it does not ‘know’ which digits need to be counted. In the second layer, it ‘knows’ that these are 7s and 1s, so the rest gets discarded. On a question answering task (see Figure 9a), where we use a 24-layer model, it takes 17–20 layers for the model to ‘realize’ that ‘Santa Clara Marriott’ and ‘Stanford University’ are not relevant to the question and discard them. In that way, we go beyond attribution, characterizing instead of how the decision is being incrementally formed by the model.

We also adapt our method to measuring the im-

portance of intermediate states rather than inputs (see Figure 4). This, as we discuss later, lets us analyze which states in every layer store information crucial for making predictions and gives us extra insights about the information flow.

Contributions Our contributions are as follows:

- we analyze limitations of existing attribution-based methods, especially erasure and its approximations;
- we propose a novel approach, DIFFMASK, addressing the shortcomings and revealing how a decision is formed across network layers;
- we use DIFFMASK to analyse BERT models fine-tuned on sentiment classification and question answering.

2 Related Work

While we motivated our approach through its relation to erasure, an alternative way of looking at our approach is considering it as a *perturbation-based* method. This recently introduced class of attribution methods (Ying et al., 2019; Guan et al., 2019; Schulz et al., 2020; Taghanaki et al., 2019), instead of erasing input, injects noise. These methods can be regarded as continuous relaxations of erasure, though they are typically motivated from the information-theoretic perspective. The previous approaches use continuous gates which may be problematic when the magnitude of input changes or requires making (Gaussian) assumptions about the input distribution. This means that information about the input can still leak to the predictor. These methods are also, similarly to subset erasure, susceptible to hindsight bias. Our method uses mixed discrete-continuous gates, which can completely block the flow, and amortization to address both these issues. We compare to perturbation-based methods in our experiments.

Besides back-propagation and attention-based methods discussed in the introduction, another class of interpretation methods (Murdoch and Szlam, 2017; Singh et al., 2018; Jin et al., 2020) builds on prior work in cooperative game theory (e.g., Shapley value of Shapley (1953)). These methods are not trivial to apply to new architectures, as new architecture-specific decomposition rules need to be derived. Their hierarchical versions (e.g., Singh et al. (2018); Jin et al. (2020)) also make a strong assumption about the structure

of interaction (e.g., forming a tree) which may affect their faithfulness.

There is a large body of literature on analyzing BERT and other Transformed-based models. For example, [Tenney et al. \(2019\)](#) and [van Aken et al. \(2019\)](#) considered probing BERT layers for a range of linguistic tasks, while [Hao et al. \(2019\)](#) analyzed the optimization surface. [Rogers et al. \(2020\)](#) provides a comprehensive overview of recent BERT analysis papers.

3 Method

We are interested in understanding how a model processes an input (e.g., a sentence) to produce an output (e.g., a vector of class probabilities). This is a complex and mostly opaque mapping realized by a stack of parameterized transformations of the input. Inspecting the parameters of the mapping or the intermediate representations themselves is all but obvious. We approach the challenge by answering two questions for every layer along with the mapping from input to output, namely, *what does the model know* and *where does it store information?*

Concretely, for each hidden layer, we first want to understand what parts of the input are necessary to arrive at the prediction. We think of this as probing what that hidden layer ‘knows’ (e.g., in our toy task, see Figure 3e, the hidden layer knows that the goal is to determine whether there are more 7s than 1s as everything else can be disregarded to arrive at the correct prediction). We reveal this information by mapping the states in a hidden layer to a masked version of the input (that is, with some tokens discarded as irrelevant). This masked input is such that, should we feed the model with it, the output would not change. We aim to mask as much as possible, thus revealing from each layer’s perspective the minimum necessary the model must read to preserve the information that layer contributes to the process of composing the original output. This offers a human-readable view of how the prediction is incrementally formed (e.g., in Figure 9a and 9b our method highlights that low layers predict that some tokens such as determinants or punctuation can be completely ignored while potential answer spans have to be kept; conversely, higher layers can make a more refined prediction to mask spans that do not contain the answer). Second, we want to know where the model stores information that is necessary for the prediction. This gives us insights

into its encoding process. Revealing this kind of information requires a minor modification to our framework, in particular, we need only change the objective of the probe. Instead of probing a hidden state for unnecessary inputs, we probe it for its relevance towards the original output. If a state can be masked-out without impact on the output, it most likely does not store information that is important from that layer onward. See Figure 7b for an example in sentiment classification, towards the top of the stack, information is eventually stored in a single state.

3.1 Masking inputs

At a conceptual level, we may think of a neural network model as a stack of transformations of an input towards an output. We use $f(x; \theta)$ to denote this entire computation, where $x = \langle x_1, \dots, x_n \rangle$ denotes an input (i.e., a sequence of embedded tokens), and θ denotes the model’s trainable parameters, which are given and fixed for the purpose of interpretation. DIFFMASK builds on the notion of erasure, whereby tokens that can be dropped without affecting the output are regarded as unnecessary. However, rather than searching through the space of alternative inputs for those that preserve the output, we probe hidden states, at different layers, for which tokens can be masked-out. On the one hand, this addresses erasure’s poor scalability (i.e., the space of masked inputs grows exponentially in sequence length). On the other hand, probing hidden states for what they know overcomes erasure’s hindsight bias.

In DIFFMASK, for an input x (also denoted $h^{(0)}$), we do a forward pass with the trained model obtaining the output $y = f(x; \theta)$ as well as all of the model’s intermediate hidden states $\langle h^{(1)}, \dots, h^{(L)} \rangle$. We then probe the model, at different hidden layers, for unnecessary inputs using a shallow prediction model. This *interpreter* model takes hidden states up to a certain layer ℓ and outputs a binary mask $z = \langle z_1, \dots, z_n \rangle$ indicating which input tokens are necessary and which can be disregarded. To appreciate whether the masked input $\hat{x} = \langle \hat{x}_1, \dots, \hat{x}_n \rangle$ is sufficient, we re-feed the model with it and compute the output $\hat{y} = f(\hat{x}; \theta)$. To avoid making changes to the computation graph of $f(\cdot; \theta)$ and to avoid changing the distribution of input length, rather than dropping tokens, we ‘mask’ them. Masking, however, as in multiplication by *zero*, makes a strong assumption about

the geometry of the feature space, in particular, it assumes that the zero vector bears no information. Instead, we replace some of the inputs by a learned baseline vector b , i.e.,

$$\hat{x}_i = z_i \cdot x_i + (1 - z_i) \cdot b. \quad (1)$$

Concretely, the interpreter model consists of $L + 1$ classifiers, the ℓ th of which conditions on the stack of hidden states $\langle h^{(0)}, \dots, h^{(\ell)} \rangle$ to predict binary ‘votes’ $v^{(\ell)} = g^{(\ell)}(h^{(0)}, \dots, h^{(\ell)}; \phi)$ towards keeping or masking input tokens. For a given depth ℓ , the interpreter decides to mask x_i out as soon as $v_i^{(k)} = 0$ for some $k \leq \ell$. That is, in order to deem x_i unnecessary, it is sufficient to do so based on any subset of hidden states up until $h^{(\ell)}$. We realize this by aggregating binary votes via a product

$$z_i = \prod_{k=0}^{\ell} v_i^{(k)}. \quad (2)$$

The precise parameterization of $g(\cdot; \phi)$ is discussed in Appendix A.

Clearly, there is no direct supervision to estimate the parameters ϕ of the probe and the baseline b , thus we borrow erasure’s conceptual objective, namely, we train the probe to mask-out as many input tokens as possible constrained to keeping $f(\hat{x}; \theta) \approx f(x; \theta)$. Where $f(\cdot; \theta)$ parameterizes a likelihood, we measure changes to the output in terms of Kullback-Leibler divergence.¹ As constrained optimization is generally intractable, in Section 3.3 we resort to Lagrangian relaxation and stochastic gradient-based optimization. See Figure 1 for an overview of DIFFMASK.

Finally, deterministically predicting a binary mask calls for a discontinuous activation, such as a threshold function, for which gradients are not well defined. To enable gradient-based learning, we employ stochastic masks as well as a relaxation to binary variables (Section 3.3) that admits differentiable sampling while retaining *sparsity*, in particular, producing true zeros.

3.2 Masking hidden states

To reveal which hidden states store information necessary for realizing the prediction, we modify the probe slightly. Again, for a given depth ℓ , we condition on the stack of states up until and including $h^{(\ell)}$, and again we have a classifier that predicts

¹Where $f(\cdot; \theta)$ does not admit a probabilistic interpretation, a distance can be used.

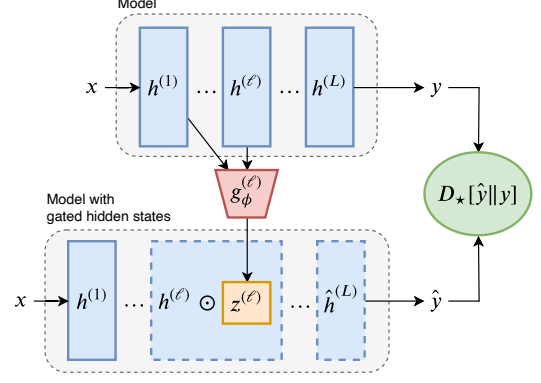


Figure 4: Overview of DIFFMASK to inspect the importance of hidden units. We take hidden states up to layer ℓ from a model (top) and feed them to a classifier g that predicts a mask $z^{(\ell)}$. We use this to mask states of the ℓ th layer and re-compute the forward pass from that point on (bottom). The classifier g is trained to mask as much of $h^{(\ell)}$ as possible without changing the output (minimizing a divergence D_\star).

a mask $z^{(\ell)} = g^{(\ell)}(h^{(0)}, \dots, h^{(\ell)}; \phi)$. This time, however, we use the mask to replace some of the *states* in $h^{(\ell)} = \langle h_1^{(\ell)}, \dots, h_n^{(\ell)} \rangle$ by a layer-specific baseline vector $b^{(\ell)}$, i.e.,

$$\hat{h}_i^{(\ell)} = z_i^{(\ell)} \cdot h_i^{(\ell)} + (1 - z_i^{(\ell)}) \cdot b^{(\ell)}. \quad (3)$$

The resulting state $\hat{h}^{(\ell)}$ is used to re-compute every subsequent hidden state, $\hat{h}^{(\ell+1)}, \dots, \hat{h}^{(L)}$, as well as the output, which we denote by \hat{y} . To the extent \hat{y} approximates the original output $y = f(x; \theta)$ well, we deem the states masked by $z^{(\ell)}$ unnecessary.

Parameter estimation for the probe and baselines is done in a similar way as before, namely, we aim to mask-out as many hidden states as possible constrained to keeping $\hat{y} \approx y$ as measured by a divergence of choice. See Figure 4 for an overview of this variant of DIFFMASK and Section A for the specification of $g(\cdot; \phi)$.

3.3 Parameter estimation

In this section we describe how to estimate the parameters ϕ of the probe as well as the baselines. For ease of notation and without loss of generality, we focus on the variant of DIFFMASK where we mask inputs (Section 3.1). Inspired by erasure, for each input x , we would like to mask-out as much of it as possible without changing the output of the model, that is, finding a mask z with as many entries set to 0 as possible and still have $f(\hat{x}; \theta) = f(x; \theta)$. Unlike erasure, rather than combinatorial search, we frame this as a learning problem. That is, we treat

z as prediction realised by an *interpreter network* $g(\cdot; \phi)$ which is shared (i.e., *amortized*) across data points.² This rather shallow network is trained to satisfy erasure’s requirements, that is, mask as much as possible subject to keeping the prediction unchanged. We can cast this, rather naturally, in the language of constrained optimization and employ a method such as Lagrangian relaxation. In general, however, it is not possible to guarantee equality between $f(\hat{x}; \theta)$ and $f(x; \theta)$,³ thus we introduce i) a divergence $D_\star[f(\hat{x}; \theta) \| f(x; \theta)]$ to measure how much the two outputs differ, and ii) a tolerance level m within which differences are regarded as acceptable. The choice of D_\star depends on the structure of the output of the original model. For instance, for a deterministic regression model, L_2 seems a convenient choice, whereas for probabilistic classification, where $f(\cdot; \theta)$ parameterizes a categorical distribution, cross-entropy or KullbackLeibler divergence are more appropriate.

Objective A practical way to minimize the number of non-zeros predicted by g is minimizing the L_0 ‘norm’.⁴ Thus, our \mathcal{L}_0 loss is defined as the number of positions that are not masked:

$$\mathcal{L}_0(\phi, b|x) = \sum_{i=1}^n \mathbf{1}_{[\mathbb{R} \neq 0]}(z_i), \quad (4)$$

where $\mathbf{1}$ is the indicator function. We minimize \mathcal{L}_0 for all data-points in the dataset \mathcal{D} subject to a constraint that predictions from masked inputs have to be similar to the original model predictions:

$$\begin{aligned} \min_{\phi, b} \quad & \sum_{x \in \mathcal{D}} \mathcal{L}_0(\phi, b|x) \\ \text{s.t.} \quad & D_\star[\hat{y} \| y] \leq m \quad \forall x \in \mathcal{D}, \end{aligned} \quad (5)$$

where $\hat{y} = f(\hat{x}; \theta)$ and $y = f(x; \theta)$. Since non-linear constrained optimisation is generally intractable, we employ Lagrangian relaxation (Boyd et al., 2004) optimizing instead

$$\max_{\lambda} \min_{\phi, b} \sum_{x \in \mathcal{D}} \mathcal{L}_0(\phi, b|x) + \lambda(D_\star[\hat{y} \| y] - m), \quad (6)$$

²This is reminiscent of how inference networks amortize prediction of local variational factors in a variational auto-encoder.

³Since $f(\cdot; \theta)$ is a smooth function a minimal change in its input cannot produce the exact same output.

⁴ L_0 , denoted $\|z\|_0$ and defined as $\#(i|z_i \neq 0)$, is the number of non-zeros entries in a vector. Contrary to L_1 or L_2 , L_0 is not a homogeneous function and, thus, not a proper norm. Contemporary literature, however, with some abuse of terminology, refers to it as a norm and we do so as well to avoid confusion.

where $\lambda \in \mathbb{R}_{\geq 0}$ is the positive Lagrangian multiplier. Although Lagrangian relaxation allows a practical approach to constrained optimization, this objective is not differentiable with respect to ϕ and b , and thus standard stochastic gradient descent methods cannot be employed. That is because i) L_0 is non-differentiable, and ii) to have $g(\cdot; \phi)$ output binary masks we need a non-differentiable output activation such as the step function.

Stochastic masks To estimate the parameters of the probe via gradient-based optimization, we cannot have $g(\cdot; \phi)$ predict *discrete* masks deterministically. Though proxy (biased) gradients do exist (e.g., deterministic straight-through (Bengio et al., 2013)), they lack theoretical support. A better understood strategy is to give binary variables stochastic treatment and compute the objective in expectation. This requires a simple change to $g_i^{(\ell)}(\cdot; \phi)$, namely, rather than directly predicting vote $v_i^{(\ell)}$, it parameterizes a Bernoulli distribution from which we then sample a vote in order to compose a mask z . Computing the objective in expectation addresses both sources of non-differentiability, but introduces a difficulty, namely, assessing the loss and the constraint for every configuration of $z \in \{0, 1\}^n$ is intractable. The intractability of the expectation forces us to resort to gradient estimation, e.g. via REINFORCE (Williams, 1992), which can suffer from high variance as we demonstrate in Section 4. Instead, we employ a relaxation to binary variables that admits sampling through a differentiable reparameterization while retaining *sparsity* (Louizos et al., 2018), in particular, producing true zeros.

Sparse relaxation Instead of sampling binary votes from Bernoulli distributions, we sample votes from Hard Concrete distributions (Louizos et al., 2018), a mixed discrete-continuous distribution over the closed interval $[0, 1]$. The Hard Concrete distribution, which we review in Appendix B, assigns density to continuous outcomes in the open interval $(0, 1)$ and non-zero mass to exactly 0 and exactly 1. A particularly appealing property of this distribution is that sampling can be done via a differentiable reparameterization (Rezende et al., 2014; Kingma and Welling, 2014). In this way, the \mathcal{L}_0 loss in Equation 4 becomes an expectation

$$\mathcal{L}_0(\phi, b|x) = \sum_{i=1}^N \mathbb{E}_{p_\phi(z_i|x)} [z_i \neq 0]. \quad (7)$$

whose gradient can be estimated via Monte Carlo sampling without the need for REINFORCE and without introducing biases. We did modify the original Hard Concrete, though only so slightly, in a way that it gives support to samples in the half-open interval $[0, 1)$, that is, with non-zero mass only at 0. That is because we need only distinguish 0 from non-zero, and the value 1 is not particularly important.⁵

Latent rationales There is a stream of work on learning interpretable models by means of extracting latent rationales (Lei et al., 2016; Bastings et al., 2019). Some of the techniques underlying DIFFMASK are related to that line of work, but overall we approach very different problems. Lei et al. (2016) use REINFORCE to minimize a downstream loss computed on masked inputs, where the masks are binary and latent. They employ L_0 regularization to solve the task while conditioning only on small subsets of the input regarded as a *rationale* for the prediction. To the same end, Bastings et al. (2019) minimize downstream loss subject to constraints on expected L_0 using a variant of the sparse relaxation of Louizos et al. (2018). In sum, they employ stochastic masks to learn an interpretable model which they learn by minimizing a downstream loss subject to constraints on L_0 , we employ stochastic masks to interpret an existing model and for that we minimize L_0 subject to constraints on that model’s downstream performance.

4 Experiments

The goal of this work is to uncover a *faithful* interpretation of an existing model, i.e. revealing, as accurately as possible, the process by which the model arrives at the prediction. Human-provided labels will not help us in demonstrating this (e.g., human rationales (Camburu et al., 2018; DeYoung et al., 2019)), as humans cannot judge if an interpretation is faithful (Jacovi and Goldberg, 2020). On the contrary, one is often interested in using such attribution methods to uncover pathologies (or biases) in models or hidden biases in the data. Evaluating faithfulness is challenging, as ground-truth is not known on real tasks and with real models. Our strategy is to i) show the effectiveness of DIFFMASK in a controlled setting where ground-truth is available (Section 4.1); ii) test the effectiveness

⁵Only a true 0 is guaranteed to completely mask an input out, while any non-zero value, however small, may leak some amount of information.

of our relaxation for learning discrete masks (on a real model, Section 4.2.1); iii) demonstrate that the method is stable and that accuracy does not degrade due to masking (Section 4.2.2). Once we have established that DIFFMASK can be trusted, we use it to analyse BERT-based models fine-tuned on sentiment classification (Sections 4.2.3–4.2.6), where we also contrast its attributions with those of other methods, and on question answering (Section 4.3).

4.1 Toy task

To help establish the faithfulness of DIFFMASK we use it to analyse a model for which the gold-truth attributions are known. Our toy task is defined as follows: given a sequence x of digits (i.e., $0 \leq x_i \leq 9$), and a query $\langle n, m \rangle$ about two digits, determine whether there are more n than m in x . We generate sequences of varying length (up to 10 digits long) sampling each element independently: with 50% probability, we draw uniformly n or m and, with 50% probability, we draw uniformly from the remaining digits. We generate 10k data-points, keeping 10% of them for validation.⁶ Intuitively, solving the task is very easy: a model has to track the occurrences of n and m , ignoring all the other inputs.

Model We implement a shallow model. It consists of an embedding layer of dimensionality 64. Then, the embedded query and input are concatenated and fed to a single-layer feed-forward NN, followed by a single-layer unidirectional GRU (Cho et al., 2014).⁷ The classification is done by a linear classifier that acts on the last hidden state of the GRU. Unsurprisingly the model solves the task almost perfectly (accuracy on validation is $> 99\%$).

Ground-truth We designed a model for which the ground-truth can be identified. In particular, input states are designed such that they store embeddings for the query (n and m) and the corresponding digit x_i . After the feed-forward layer, hidden states need no longer store the identity of the digit (i.e., x_i) but simply whether x_i is n , m , or other. We verify this by plotting the distribution of hidden states (which we set to dimension 2 with

⁶The total number of possible input sequences for this task is $> 10^{10}$. Thus, a model that solves the task cannot simply memorize the training set.

⁷We use a feed-forward NN to incorporate the query information, rather than another GRU layer, to ensure that counting cannot happen in the first layer. This helps us define the ground-truth for the method.

Methods	D_{KL}	D_{JS}
Erasure	— *	0.26
Sundararajan et al. (2017)	0.48	0.14
Schulz et al. (2020)	1.21	0.19
Guan et al. (2019)	0.78	0.22
DIFFMASK	0.00	0.00

Table 1: Toy task: average divergence in nats between the *ground-truth* attributions and those different methods assigned to hidden states in the validation set. *Erasure produces a delta distribution that does not share support with the *ground-truth*.

the purpose of having a bottleneck and a clear visualization) in Figure 12 in Appendix D, where we observe linear separation between states of digits in the query and states of digits not in the query. This confirms that the role of the feed-forward layer is to decide which digits to keep, while the GRU must figure out which one occurred the most. In sum, we know the prediction must be attributed uniformly to *all* of the input positions where x_i is n or m .

Approaches We compare DIFFMASK to integrated gradient (Sundararajan et al., 2017), as one of the most widely used attribution methods, as well as the perturbation methods by Schulz et al. (2020) and Guan et al. (2019). We also perform erasure by searching exhaustively for masked inputs that yield the same prediction.

Results We start with an example of *input attributions*, see Figure 3, which illustrates how DIFFMASK goes beyond input attribution as typically known.⁸ The attribution provided by erasure (Figure 3a) is not informative: the search in this case, and in all other examples in the test set, finds a single digit that is sufficient to maintain the original prediction and discards all the other inputs. The perturbation methods by Schulz et al. (2020) and Guan et al. (2019) (Figure 3b and 3d) are also over-aggressive in pruning. They assign low attribution to some items in the query even though those had to be considered when making the prediction. Integrated gradient (Figure 3c) assigns high importance to the digits that appear in the query. Differently from other methods, our DIFFMASK reveals input attributions conditioned on different levels of depth. Figure 3e shows both input attribu-

⁸To enable comparison across methods, the attributions in this Section are re-normalized to 1 (whereas DIFFMASK gates before normalization tend to be 0 or 1).

Metrics	REINFORCE+	DIFFMASK
Precision	78.13	87.12
Recall	86.40	91.68
F_1	77.31	87.15
Sparsity	78.57	76.58
Optimality	15.67	45.33

Table 2: Sentiment classification: optimization with DIFFMASK and REINFORCE (with a moving average baseline for variance reduction) not amortised against erasure exact search. All metrics are computed at token level where optimality is measured at sentence level.

tions according to the input itself (left) and according to the hidden layer (right). It reveals that at the embedding layer there is no information regarding what part of the input can be erased: attribution is uniform over the input sequence. After the model has observed the query, hidden states predict that masking input digits other than n and m will not affect the final prediction: attribution is uniform over digits in the query. This reveals the role of the feed-forward layer as a filter for positions relevant to the query. Other methods do not allow for this type of inspection. These observations are consistent across the entire test set. For *attribution to hidden states* (i.e., the output of the feed-forward layer) we can compare all methods in terms of how much their attributions resemble the ground-truth across the test set. Table 1 shows how the different approaches deviate from the gold-truth in terms of Kullback-Leibler (D_{KL}) and JensenShannon (D_{JS}) divergences.⁹ Our method, unlike other methods, achieves perfect scores on the test set.

4.2 Sentiment Classification

We turn now to a real task and analyze a standard BERT_{BASE} model fine-tuned for sentiment classification on the Stanford Sentiment Treebank (SST; Socher et al., 2013). It consists of a pre-trained BERT_{BASE} followed by a pooling layer (which simply takes the hidden state of the first token) and a linear classifier. The model is trained with the cross-entropy loss to predict one of the 5 sentiment classes: very negative, negative, neutral, positive, and very positive. We then apply our DIFFMASK

⁹We use $D_{KL}[p||q]$ where p is the *ground-truth* attribution distribution and q the attribution distribution of a method we want to compare with. D_{KL} is an asymmetric divergence where D_{JS} is a symmetric version of it. Both measure how much two distribution differ (i.e., lower the value more similar the two distributions are).

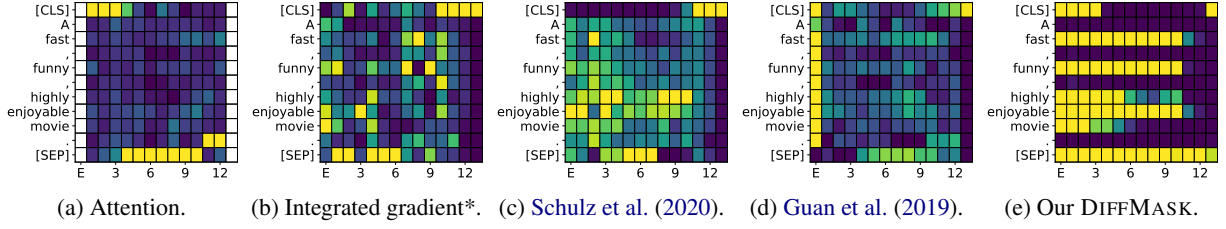


Figure 5: Sentiment classification: comparison between attribution method for hidden layers w.r.t. the predicted label. All plots are normalized per-layer by the largest attribution. Attention heatmap is obtained max pooling over heads and averaging across positions. *By Sundararajan et al. (2017).

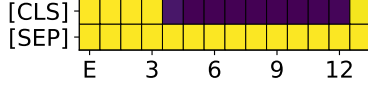


Figure 6: Average keep probability for every hidden layer of start and end-of-sentence tokens.

for both input attribution (i.e., as function of hidden states at different depths) and hidden state attribution. We train DIFFMASK with a KL divergence constraint $D_{\text{KL}}[y||\hat{y}]$.¹⁰ Hyperparameters are reported in Appendix C.1.

4.2.1 Erasure search as learning masks

Before diving into analysis of the sentiment model, we would like to demonstrate we can learn informative subsets through our differentiable relaxations. In order to do this, we need to have access to the ground-truth. We do not have it for our full approach, but we can obtain it when we do not use amortization (i.e. when all Hard Concrete parameters are learned for a specific example rather than predicted from the BERT states). In that case an optimal solution (or a set of equally good optimal solutions) is provided by erasure. We compare DIFFMASK to REINFORCE (Williams, 1992) with a moving average baseline for variance reduction. Since erasure requires exact search, and it is unfeasible for long sequences, we evaluate here using only sentences up to 25 words ($\sim 54\%$ of the data). In Table 2 we show the superiority of DIFFMASK to REINFORCE. Both achieved a comparable level of sparsity while our method reaches an optimal solution much more often than REINFORCE (45% of the times vs 16%) and is, on average, closer to an optimal solution (87% F_1 vs 77% F_1).

4.2.2 Maintaining prediction and stability

Now, we get back to the fully amortized DIFFMASK approach and verify that there is no perfor-

mance degradation when applying masking. Indeed, the macro F_1 score of the model on validation moved from 37.9% to 38.3% while masking 46.3% input tokens and to 38.9% while masking 67.6% hidden states. The explanation provided by DIFFMASK are also stable. Across 5 independent runs with different seeds, the standard deviation of input attributions is 0.0553 and for hidden state attributions is 0.0302 (averaged across the validation set).

4.2.3 Comparisons

Our previous experiments were aimed primarily at showing that DIFFMASK can be trusted. Now, we finally turn to using DIFFMASK to actually analyze the sentiment model.

While previous techniques (e.g., integrated gradient) do not let us test what a model ‘knows’ in a given layer (i.e. attribution to input conditioned on a layer), they can be used to perform attribution to hidden layers. In Figure 5 we compare our method with recent techniques in that regime. In Figure 13 in Appendix D we show an additional example.

Raw attention (Figure 5a) does not seem to highlight any significant patterns in that example except that start and end of sentence tokens ([CLS] and [SEP], respectively) receive more attention than the rest.¹¹ All the other methods correctly highlight the last hidden state of the [CLS] token as important. Its importance is due to the top-level classifier using the [CLS] hidden state. The methods by Schulz et al. (2020) and Guan et al. (2019) assign slightly higher importance to hidden states corresponding to ‘highly’ and ‘enjoyable’, whereas it is hard to see any informative patterns in heatmaps provided by integrated gradient. Our method assigns much sharper attribution. In Figure 5e it is

¹⁰We do not update BERT parameters when optimizing DIFFMASK. Memory and computation overhead is negligible.

¹¹Voita et al. (2019b) and Michel et al. (2019) pointed out that many Transformer heads play no or minor role, so it may be possible to obtain more informative attributions if the ‘useless’ heads are disregarded.

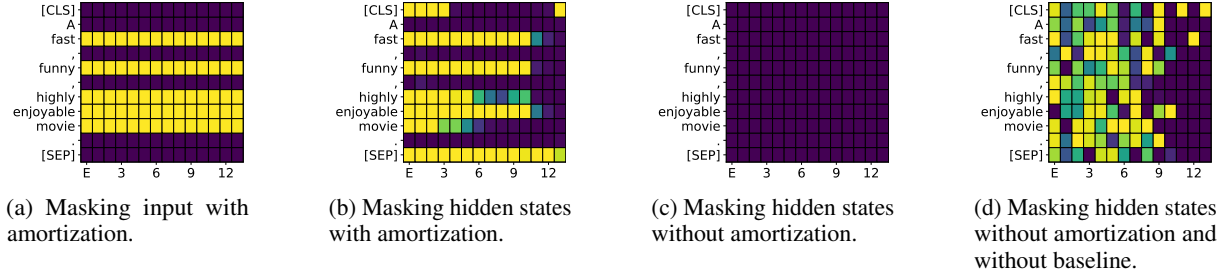


Figure 7: Sentiment classification: highlighting difference between input and hidden state attributions in (a) and (b), and ablation study on amortization in (b), (c) and (d).

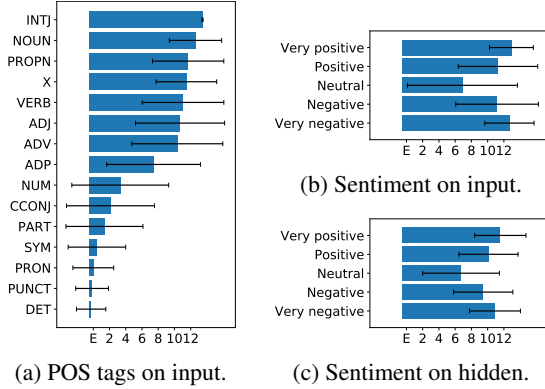


Figure 8: Sentiment classification: average number of layers that predict to keep input tokens or hidden states on validation set. (a) shows average predictions on input aggregating by part-of-speech tag (POS) where (b) and (c) by token level sentiment annotations.

evident that hidden states associated with punctuation can be completely dropped, while the rest needs to be kept. Importantly, with DIFFMASK, the zero attribution has a very clear interpretation: when DIFFMASK masks a hidden state, that state is not used for prediction (i.e in layers higher up in the model).

4.2.4 Analysis

The hidden state attribution we have done so far tells us if a state stores important information. Now, we contrast it to input attribution, which, with DIFFMASK, shows what the model ‘knows’ at a given layer. The two attributions are shown in Figure 7a and 7b. The situation here seems relatively straightforward. From Figure 7a we see that the model, even in the bottom layers, knows that the punctuation and both separators can be dropped from the input. This contrasts with hidden states attribution (Figure 7b) which indicates that the separator states (especially [SEP]) are very important. By putting this information together, we can hypothesize that the separator is used to aggregate informa-

tion from the sentence, relying on self-attention. In fact, this aggregation is still happening in layer 11; at the very top layers, states corresponding to all non-separator tokens can be dropped. In Figure 6, we confirm the separators are important across the dataset and not only on this example. In Figure 8a we instead aggregate input attributions according to part-of-speech tags. With this sentiment model, determinants, punctuation, and pronouns can be completely discarded from the input while adjective and nouns should be kept.

4.2.5 Human labels

While we cannot use human labels to evaluate faithfulness of our method, comparing them and DIFFMASK attribution will tell us whether the sentiment model relies on the same cues as humans. Specifically, we use the SST token level annotation of sentiment. In Figure 8b, we show after how many layers on average an input token is dropped, depending on its sentiment label. Figure 8c shows the same for hidden states. This suggests that the model relies more heavily on strongly positive or negative words and, thus, is generally consistent with human judgments.

4.2.6 Ablation

As argued in the introduction and shown on the toy task, many popular methods (e.g., erasure and its approximations) are over-aggressive in discarding inputs and hidden units. Amortization is a fundamental component of DIFFMASK and is aimed at addressing this issue. In Figure 7 we show how our method behaves when ablating amortization and thus optimizing on a single example instead. Noticeable, our method converges to masking out all hidden states at any layer (Figure 7c). This happens as it learns an *ad hoc* baseline just for that example. When we ablate both amortization and baseline learning (Figure 7d), the method struggles to uncover any meaningful patterns. This highlights how

both core components of our method are needed in combination with each other.

4.3 Question Answering

We turn now to extractive question answering where we analyse a fine-tuned BERT_{LARGE} model trained on the Stanford Question Answering Dataset v1.1 (SQUAD; Rajpurkar et al., 2016). It consists of a pre-trained BERT_{LARGE} encoder followed by two independent linear classifiers that predict the beginning and the end of the span that contains the answer in the document. The model is fine-tuned to minimize the cross-entropy error for span prediction, while DIFFMASK minimizes L_0 subject to a constraint on $D_{KL}[y||\hat{y}]$.¹⁰ Hyperparameters are reported in Appendix C.2.

4.3.1 Comparison to other methods

As we do not have access to the ground-truth, we start by contrasting DIFFMASK qualitatively to other attribution methods on a few examples. We highlight some common pitfalls that afflict other methods (such as the hindsight bias) and how DIFFMASK overcomes those. This helps demonstrate our method’s faithfulness to the original model. In addition, we discuss how DIFFMASK explanations provide deeper insight into how predictions are formed.

Figure 2 shows input attributions by different methods on an example from the validation set. Erasure (Figure 2e), as expected, does not provide useful insights, it essentially singles out the answer discarding everything else including the question. This cannot be faithful and is a simple consequence of erasure’s hindsight bias: when only the span that contains the answer is presented as input, the model predicts that very span as the answer, but this does not imply that the model ignores everything else when presented with the complete document as input. The methods of Schulz et al. (2020) and Guan et al. (2019) optimize attributions on single examples and thus also converge to assigning high importance mostly to words that support the current prediction and that indicate the question type. Integrated gradient does not seem to highlight any discernible pattern, which we speculate is largely because a zero baseline is not suitable for word embeddings. Choosing a more adequate baseline is not straightforward and remains an important open issue (Sturmfels et al., 2020). Note that without amortization, DIFFMASK closely approximates erasure (as demonstrated in Section 4.2.1 for SST),

and indeed Figure 2f is another example of the hindsight bias which prevents us from gaining insights about the model.

Differently from all other methods, our DIFFMASK probes the network to understand what it ‘knows’ about the input-output mapping in different layers. In Figure 2d we show the expectation of keeping input tokens conditioned on any one of the layers in the model to make such predictions. Our input attributions highlight that the model, in expectation across layers, *wants* to keep words in the question as well as all potential candidate answers, but that eventually, the most important spans are in the question and the answer itself.

4.3.2 Analysis

Having provided additional evidence that DIFFMASK explanations are faithful, we proceed to uncovering patterns in how the model processes inputs. We start by asking ourselves, or rather DIFFMASK, **which tokens does the model keep?** In Figure 9a and 9b we visualize the expectations of keeping the input tokens with respect to each of BERT’s layers on two different questions about the same passage. For that example, the model seems to ignore almost all determinants, prepositions, and conjunctions to perform its predictions. To better investigate the role of different parts of speech (POS), we aggregate statistics over the entire validation set in Figure 10. It indeed emerges that those parts of speech are largely ignored by the model, while nouns and proper nouns are often kept. We argue that due to the pre-training objective, BERT could infer well missing parts of the input, especially if they are trivial to infer (e.g., as prepositions or determiners in many cases). In contrast, in Figure 9a, we can see that takes 17–20 layers for the model to ‘realize’ that ‘*Santa Clara Marriott*’ and ‘*Stanford University*’ are not relevant to the question and discard them.

Similarly to sentiment classification, the [CLS] tokens appear not useful. Conversely, the [SEP] tokens are important (at least according to bottom layers). Notice that, in this task, the [SEP] token is also used as a separator between the question and the passage, and hence indicates where the questions end. However, at ~ 12 th layer, the model is already confident what the possible answers could be, so these tokens are no longer needed.

Unsurprisingly, in both examples, all layers choose to keep the originally predicted answer spans. Across the validation set, this is happen-

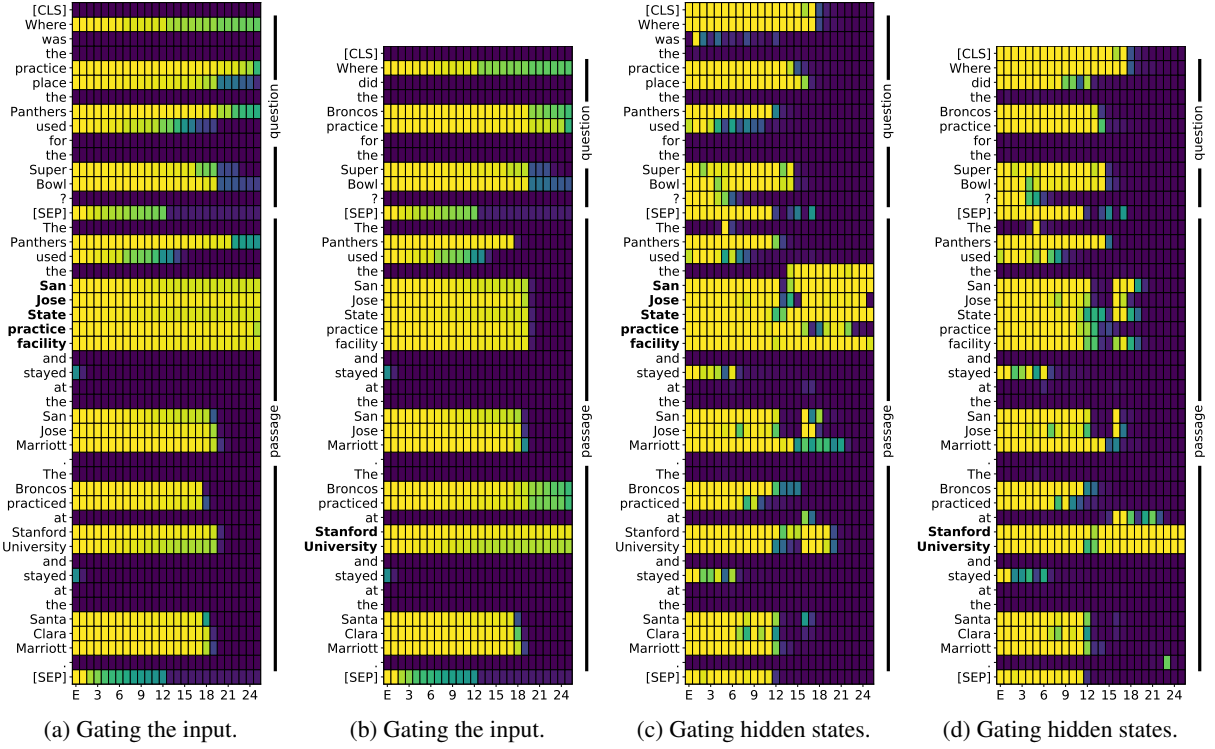


Figure 9: Expectation predicted by DIFFMASK to keep the inputs in (a) and (b) or hidden states in (c) and (d) on two different questions on the same paragraph. The correct answers is highlighted in bold.

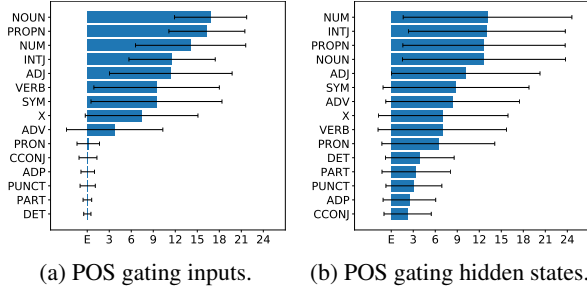


Figure 10: Question answering: average number of layers that predict to keep input tokens (a) or hidden states (b) aggregating by part-of-speech tag (POS) on validation set.

ing in 94% of cases. Incrementality in processing the data is much more evident here than on the sentiment task. For example, at least 18 layers are needed to decide to drop any named entity. At top layers (e.g., top 4), the model can drop almost everything except for the answer, indicating that the model has already converged to the decision. Higher layers also still vote to keep parts of the question (e.g., ‘Where’), presumably because it is fundamental for selecting the answer type. Key named entities in the questions are kept as well, while the question mark is always dropped: it is present in every question so does not carry any in-

formation. Our observation that higher layers are more predictive is in line with findings of Kovaleva et al. (2019). They pointed out that final layers of BERT change most and are more task specific.

Where is the information stored? In Figure 9c and 9d we visualize the expectations of keeping hidden states across layers predicted by DIFFMASK on two different questions, but for the same passage. Differently from deciding which input tokens to drop (as in Figure 9a and 9b), masking hidden states sheds light on which hidden states store important information. As an example, the model seems to use the hidden states aligned with the determiner ‘the’ in proximity of the answer span in Figure 9c. Although determinants can be completely ignored as inputs, their hidden states are actually used by the model. It is consistent with findings in Voita et al. (2019a) which show that frequent tokens, such as determiners, accumulate contextual information. Statistics aggregated for different part-of-speech tags across the validation set (Figure 10b) confirms this intuition.

All layers > 21 are voting to drop every state except the ones corresponding to the answer span. These contain information needed at the top layer for classification while all the others can indeed be

removed, without affecting the model prediction. In contrast, intermediate layers 12–18 seem to be still considering different span options, as they are still active on all plausible spans (i.e., names of locations).

5 Conclusion

The recent developments in expressivity and efficacy of complex deep neural networks have come at the expense of interpretability. While systematically erasing inputs to determine how a model reacts leads to a neat interpretation, it comes with many issues such as an exponential computational time complexity and susceptibility to the hindsight bias: if a word can be dropped from the input, it does not necessarily imply that it is not used by the model. We have introduced a new *post hoc* interpretation method which learns to completely remove subsets of inputs or hidden states through masking. We circumvent an intractable search by learning an end-to-end differentiable prediction model. To circumvent the hindsight bias problem, we probe the model’s hidden states at different depths and amortize predictions over the training set.

We validate the faithfulness of DIFFMASK in a controlled artificial experiment pointing more clearly to some flaws of other attribution methods. DIFFMASK without amortization was also shown to approximate erasure well in a real task (SST) and to outperform REINFORCE in doing so both in terms of performance and stability across runs. Having established that DIFFMASK can be trusted, we used it to study BERT-based models on sentiment classification and question answering. Our method sheds light on what different layers ‘know’ about the input and where information about the prediction is stored in different layers.

Acknowledgements

Authors want to thank Christos Baziotis, Elena Voita, Dieuwke Hupkes, and Naomi Saphra for helpful discussions. This project is supported by SAP Innovation Center Network, ERC Starting Grant BroadSem (678254), the Dutch Organization for Scientific Research (NWO) VIDI 639.022.518, and the European Union’s Horizon 2020 research and innovation programme under grant agreement No 825299 (Gourmet).

References

- Yossi Adi, Einat Kermany, Yonatan Belinkov, Ofer Lavi, and Yoav Goldberg. 2017. Fine-grained analysis of sentence embeddings using auxiliary prediction tasks. *Proceedings of ICLR*.
- Betty van Aken, Benjamin Winter, Alexander Löser, and Felix A Gers. 2019. How does bert answer questions? a layer-wise analysis of transformer representations. In *Proceedings of the 28th ACM International Conference on Information and Knowledge Management*, pages 1823–1832.
- Sebastian Bach, Alexander Binder, Grégoire Montavon, Frederick Klauschen, Klaus-Robert Müller, and Wojciech Samek. 2015. On pixel-wise explanations for non-linear classifier decisions by layer-wise relevance propagation. *PloS one*, 10(7).
- David Baehrens, Timon Schroeter, Stefan Harmeling, Motoaki Kawanabe, Katja Hansen, and Klaus-Robert Müller. 2010. How to explain individual classification decisions. *Journal of Machine Learning Research*, 11(Jun):1803–1831.
- Joost Bastings, Wilker Aziz, and Ivan Titov. 2019. [Interpretable neural predictions with differentiable binary variables](#). In *Proceedings of the 57th Annual Meeting of the Association for Computational Linguistics*, pages 2963–2977, Florence, Italy. Association for Computational Linguistics.
- Yonatan Belinkov and James Glass. 2019. Analysis methods in neural language processing: A survey. *Transactions of the Association for Computational Linguistics*, 7:49–72.
- Yoshua Bengio, Nicholas Léonard, and Aaron Courville. 2013. Estimating or propagating gradients through stochastic neurons for conditional computation. *arXiv preprint arXiv:1308.3432*.
- Stephen Boyd, Stephen P Boyd, and Lieven Vandenberghe. 2004. *Convex optimization*. Cambridge university press.
- Oana-Maria Camburu, Tim Rocktäschel, Thomas Lukasiewicz, and Phil Blunsom. 2018. e-snli: Natural language inference with natural language explanations. In *Advances in Neural Information Processing Systems*, pages 9539–9549.
- Kyunghyun Cho, Bart van Merriënboer, Caglar Gulcehre, Dzmitry Bahdanau, Fethi Bougares, Holger Schwenk, and Yoshua Bengio. 2014. [Learning phrase representations using RNN encoder-decoder for statistical machine translation](#). In *Proceedings of the 2014 Conference on Empirical Methods in Natural Language Processing (EMNLP)*, pages 1724–1734, Doha, Qatar. Association for Computational Linguistics.
- Jay DeYoung, Sarthak Jain, Nazneen Fatema Rajani, Eric Lehman, Caiming Xiong, Richard Socher, and Byron C Wallace. 2019. Eraser: A benchmark to

- evaluate rationalized nlp models. *arXiv preprint arXiv:1911.03429*.
- Shi Feng, Eric Wallace, II Grissom, Mohit Iyyer, Pedro Rodriguez, Jordan Boyd-Graber, et al. 2018. Pathologies of neural models make interpretations difficult. *EMNLP*.
- Yoav Goldberg. 2017. Neural network methods for natural language processing. *Synthesis Lectures on Human Language Technologies*, 10(1):1–309.
- Chaoyu Guan, Xiting Wang, Quanshi Zhang, Runjin Chen, Di He, and Xing Xie. 2019. Towards a deep and unified understanding of deep neural models in nlp. In *International Conference on Machine Learning*, pages 2454–2463.
- Suchin Gururangan, Swabha Swayamdipta, Omer Levy, Roy Schwartz, Samuel R Bowman, and Noah A Smith. 2018. Annotation artifacts in natural language inference data. *arXiv preprint arXiv:1803.02324*.
- Yaru Hao, Li Dong, Furu Wei, and Ke Xu. 2019. [Visualizing and understanding the effectiveness of BERT](#). In *Proceedings of the 2019 Conference on Empirical Methods in Natural Language Processing and the 9th International Joint Conference on Natural Language Processing (EMNLP-IJCNLP)*, pages 4143–4152, Hong Kong, China. Association for Computational Linguistics.
- Kenneth Holstein, Jennifer Wortman Vaughan, Hal Daumé III, Miro Dudík, and Hanna Wallach. 2019. Improving fairness in machine learning systems: What do industry practitioners need? In *Proceedings of the 2019 CHI Conference on Human Factors in Computing Systems*, pages 1–16.
- Alon Jacovi and Yoav Goldberg. 2020. Towards faithfully interpretable nlp systems: How should we define and evaluate faithfulness? *arXiv preprint arXiv:2004.03685*.
- Sarthak Jain and Byron C. Wallace. 2019. [Attention is not Explanation](#). In *Proceedings of the 2019 Conference of the North American Chapter of the Association for Computational Linguistics: Human Language Technologies, Volume 1 (Long and Short Papers)*, pages 3543–3556, Minneapolis, Minnesota. Association for Computational Linguistics.
- Eric Jang, Shixiang Gu, and Ben Poole. 2017. Categorical reparameterization with Gumbel-Softmax. *International Conference on Learning Representations*.
- Xisen Jin, Junyi Du, Zhongyu Wei, Xiangyang Xue, and Xiang Ren. 2020. Towards Hierarchical Importance Attribution: Explaining Compositional Semantics for Neural Sequence Models. *International Conference on Learning Representations*.
- Divyansh Kaushik and Zachary C Lipton. 2018. How much reading does reading comprehension require? a critical investigation of popular benchmarks. *Proceedings of EMNLP*.
- Been Kim. 2015. *Interactive and interpretable machine learning models for human machine collaboration*. Ph.D. thesis, Massachusetts Institute of Technology.
- Diederik P Kingma and Jimmy Ba. 2015. Adam: A method for stochastic optimization. *International Conference for Learning Representations*.
- Diederik P Kingma and Max Welling. 2014. Auto-encoding variational bayes. *Proceedings of the 2nd International Conference on Learning Representations (ICLR)*.
- Olga Kovaleva, Alexey Romanov, Anna Rogers, and Anna Rumshisky. 2019. [Revealing the dark secrets of BERT](#). In *Proceedings of the 2019 Conference on Empirical Methods in Natural Language Processing and the 9th International Joint Conference on Natural Language Processing (EMNLP-IJCNLP)*, pages 4365–4374, Hong Kong, China. Association for Computational Linguistics.
- Tao Lei, Regina Barzilay, and Tommi Jaakkola. 2016. [Rationalizing neural predictions](#). In *Proceedings of the 2016 Conference on Empirical Methods in Natural Language Processing*, pages 107–117, Austin, Texas. Association for Computational Linguistics.
- Jiwei Li, Will Monroe, and Dan Jurafsky. 2016. Understanding neural networks through representation erasure. *arXiv preprint arXiv:1612.08220*.
- Christos Louizos, Max Welling, and Diederik P Kingma. 2018. Learning Sparse Neural Networks through L_0 Regularization. *International Conference on Learning Representations (ICLR)*.
- Chris J Maddison, Andriy Mnih, and Yee Whye Teh. 2017. The concrete distribution: A continuous relaxation of discrete random variables. *International Conference on Learning Representations (ICLR)*.
- Paul Michel, Omer Levy, and Graham Neubig. 2019. Are sixteen heads really better than one? In *Advances in Neural Information Processing Systems*, pages 14014–14024.
- W James Murdoch and Arthur Szlam. 2017. Automatic rule extraction from long short term memory networks. *arXiv preprint arXiv:1702.02540*.
- Weili Nie, Yang Zhang, and Ankit Patel. 2018. A theoretical explanation for perplexing behaviors of backpropagation-based visualizations. *ICML*.
- Pranav Rajpurkar, Jian Zhang, Konstantin Lopyrev, and Percy Liang. 2016. [SQuAD: 100,000+ questions for machine comprehension of text](#). In *Proceedings of the 2016 Conference on Empirical Methods in Natural Language Processing*, pages 2383–2392, Austin, Texas. Association for Computational Linguistics.

- Danilo Jimenez Rezende, Shakir Mohamed, and Daan Wierstra. 2014. Stochastic backpropagation and approximate inference in deep generative models. *International Conference on Machine Learning (ICML)*.
- Marco Tulio Ribeiro, Sameer Singh, and Carlos Guestrin. 2016. "why should i trust you?" explaining the predictions of any classifier. In *Proceedings of the 22nd ACM SIGKDD international conference on knowledge discovery and data mining*, pages 1135–1144.
- Tim Rocktäschel, Edward Grefenstette, Karl Moritz Hermann, Tomáš Kočiský, and Phil Blunsom. 2015. Reasoning about entailment with neural attention. *arXiv preprint arXiv:1509.06664*.
- Anna Rogers, Olga Kovaleva, and Anna Rumshisky. 2020. A primer in bertology: What we know about how bert works. *arXiv preprint arXiv:2002.12327*.
- Karl Schulz, Leon Sixt, Federico Tombari, and Tim Landgraf. 2020. [Restricting the flow: Information bottlenecks for attribution](#). In *International Conference on Learning Representations*.
- Sofia Serrano and Noah A. Smith. 2019. [Is attention interpretable?](#) In *Proceedings of the 57th Annual Meeting of the Association for Computational Linguistics*, pages 2931–2951, Florence, Italy. Association for Computational Linguistics.
- Lloyd S Shapley. 1953. A value for n-person games. *Contributions to the Theory of Games*, 2(28):307–317.
- Avanti Shrikumar, Peyton Greenside, and Anshul Kundaje. 2017. Learning important features through propagating activation differences. In *Proceedings of the 34th International Conference on Machine Learning-Volume 70*, pages 3145–3153. JMLR. org.
- Karen Simonyan, Andrea Vedaldi, and Andrew Zisserman. 2013. Deep inside convolutional networks: Visualising image classification models and saliency maps. *arXiv preprint arXiv:1312.6034*.
- Chandan Singh, W James Murdoch, and Bin Yu. 2018. Hierarchical interpretations for neural network predictions. *arXiv preprint arXiv:1806.05337*.
- Leon Sixt, Maximilian Granz, and Tim Landgraf. 2019. When explanations lie: Why many modified bp attributions fail. *arXiv*, pages arXiv–1912.
- Richard Socher, Alex Perelygin, Jean Wu, Jason Chuang, Christopher D. Manning, Andrew Ng, and Christopher Potts. 2013. [Recursive deep models for semantic compositionality over a sentiment tree-bank](#). In *Proceedings of the 2013 Conference on Empirical Methods in Natural Language Processing*, pages 1631–1642, Seattle, Washington, USA. Association for Computational Linguistics.
- Pascal Sturmfels, Scott Lundberg, and Su-In Lee. 2020. Visualizing the impact of feature attribution baselines. *Distill*, 5(1):e22.
- Tony Sun, Andrew Gaut, Shirlyn Tang, Yuxin Huang, Mai ElSherief, Jieyu Zhao, Diba Mirza, Elizabeth Belding, Kai-Wei Chang, and William Yang Wang. 2019. Mitigating gender bias in natural language processing: Literature review. *arXiv preprint arXiv:1906.08976*.
- Mukund Sundararajan, Ankur Taly, and Qiqi Yan. 2017. Axiomatic attribution for deep networks. In *Proceedings of the 34th International Conference on Machine Learning-Volume 70*, pages 3319–3328. JMLR. org.
- Saeid Asgari Taghanaki, Mohammad Havaei, Tess Berthier, Francis Dutil, Lisa Di Jorio, Ghassan Hamarneh, and Yoshua Bengio. 2019. Infomask: Masked variational latent representation to localize chest disease. In *International Conference on Medical Image Computing and Computer-Assisted Intervention*, pages 739–747. Springer.
- Ian Tenney, Patrick Xia, Berlin Chen, Alex Wang, Adam Poliak, R Thomas McCoy, Najoung Kim, Benjamin Van Durme, Samuel R Bowman, Dipanjan Das, et al. 2019. What do you learn from context? probing for sentence structure in contextualized word representations. *arXiv preprint arXiv:1905.06316*.
- Tijmen Tieleman and Geoffrey Hinton. 2012. Lecture 6.5-rmsprop: Divide the gradient by a running average of its recent magnitude. *COURSERA: Neural networks for machine learning*, 4(2):26–31.
- Shikhar Vashishth, Shyam Upadhyay, Gaurav Singh Tomar, and Manaal Faruqi. 2019. Attention interpretability across NLP tasks. *arXiv preprint arXiv:1909.11218*.
- Elena Voita, Rico Sennrich, and Ivan Titov. 2019a. [The bottom-up evolution of representations in the transformer: A study with machine translation and language modeling objectives](#). In *Proceedings of the 2019 Conference on Empirical Methods in Natural Language Processing and the 9th International Joint Conference on Natural Language Processing (EMNLP-IJCNLP)*, pages 4396–4406, Hong Kong, China. Association for Computational Linguistics.
- Elena Voita, David Talbot, Fedor Moiseev, Rico Sennrich, and Ivan Titov. 2019b. [Analyzing multi-head self-attention: Specialized heads do the heavy lifting, the rest can be pruned](#). In *Proceedings of the 57th Annual Meeting of the Association for Computational Linguistics*, pages 5797–5808, Florence, Italy. Association for Computational Linguistics.
- Ronald J Williams. 1992. Simple statistical gradient-following algorithms for connectionist reinforcement learning. *Machine learning*, 8(3-4):229–256.

Thomas Wolf, L Debut, V Sanh, J Chaumond, C Delangue, A Moi, P Cistac, T Rault, R Louf, M Funtowicz, et al. 2019. Huggingfaces transformers: State-of-the-art natural language processing. *ArXiv, abs/1910.03771*.

Zhitao Ying, Dylan Bourgeois, Jiaxuan You, Marinka Zitnik, and Jure Leskovec. 2019. GNNExplainer: Generating explanations for graph neural networks. In *Advances in Neural Information Processing Systems*, pages 9240–9251.

Michael Zhang, James Lucas, Jimmy Ba, and Geoffrey E Hinton. 2019. Lookahead optimizer: k steps forward, 1 step back. In *Advances in Neural Information Processing Systems*, pages 9593–9604.

Luisa M Zintgraf, Taco S Cohen, Tameem Adel, and Max Welling. 2017. Visualizing deep neural network decisions: Prediction difference analysis. *ICLR*.

A Parameterization

To keep the probes as simple as possible, we parameterized them as bilinear functions. When masking input tokens, ‘votes’ are computed as $v^{(\ell)} = g^{(\ell)}(x, h^{(1)}, \dots, h^{(\ell)}; \phi)$ where

$$\hat{\gamma}_i^{(\ell)} = x_i^\top W_1^{(\ell)} h_i^{(\ell)} + W_2^{(\ell)}[x_i; h_i^{(\ell)}] + b^{(\ell)}, \quad (8)$$

$$\gamma_i^{(\ell)} = \frac{1}{2} \left(\hat{\gamma}_i^{(\ell)} + \frac{1}{\ell-1} \sum_{k=1}^{\ell-1} \hat{\gamma}_i^{(k)} \right), \quad (9)$$

$$v_i^{(\ell)} \sim \text{HardConcrete}(\tau, \gamma_i^{(\ell)}). \quad (10)$$

$\phi = \langle W_1^{(\ell)}, W_2^{(\ell)}, b^{(\ell)} \rangle$ are trainable parameters. See Appendix B for details about the Hard Concrete distribution including its parameterization. When masking hidden states, we use the same functional form to compute $z^{(\ell)}$ but x_i is replaced by $h_i^{(\ell)}$.

B Binary Concrete

A stretched and rectified Binary Concrete (also known as Hard Concrete) distribution is obtained applying an affine transformation to the Binary Concrete distribution (Maddison et al., 2017; Jang et al., 2017) and rectifying its samples in the interval $[0, 1]$ (see Figure 11). A Binary Concrete is defined over the open interval $(0, 1)$ (p_C in Figure 11a) and it is parameterised by a location parameter $\gamma \in \mathbb{R}$ and temperature parameter $\tau \in \mathbb{R}_{>0}$. The location acts as a logit and it controls the probability mass skewing the distribution towards 0 in case of negative location and towards 1 in case of positive location. The temperature parameter controls the concentration of the distribution. The Binary Concrete is then stretched with an affine transformation extending its support to (l, r) with $l \leq 0$ and $r \geq 1$ (p_{SC} in Figure 11a). Finally, we obtain a Hard Concrete distribution rectifying samples in the interval $[0, 1]$. This corresponds to collapsing the probability mass over the interval $(l, 0]$ to 0, and the mass over the interval $[1, r)$ to 1 (p_{HC} in Figure 11b). This induces a distribution over the close interval $[0, 1]$ with non-zero mass at 0 and 1. Samples are obtained using

$$\begin{aligned} s &= \sigma((\log u - \log(1 - u) + \gamma) / \tau) \\ z &= \min(1, \max(0, s \cdot (l - r) + r)) \end{aligned} \quad (11)$$

where σ is the Sigmoid function $\sigma(x) = (1 + e^{-x})^{-1}$ and $u \sim \mathcal{U}(0, 1)$. We point to the Appendix B of Louizos et al. (2018) for more informa-

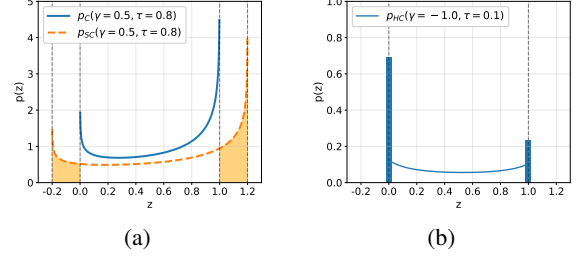


Figure 11: Binary Concrete distributions: (a) a Concrete p_C and its stretched version p_{SC} ; (b) a rectified and stretched (Hard) Concrete p_{HC} .

Model	Value
Type	BERT _{BASE} (uncased)
Layers	12
Hidden units	768
Pre-trained masking	standard
Optimizer	Adam *
Learning rate	$3 \cdot 10^{-5}$
Train epochs	50
Batch size	64
DIFFMASK	Value
Optimizer	Lookahead RMSprop **
Learning rate ϕ, t	$3 \cdot 10^{-4}$
Learning rate α	$1 \cdot 10^{-1}$
Train epochs	50
Batch size	64
Constrain	$D_{\text{KL}}[y \parallel \hat{y}] < 0.5$

Table 3: List of hyperparameters for the sentiment classification experiment. *is Kingma and Ba (2015), **is Tieleman and Hinton (2012); Zhang et al. (2019).

tion about the density of the resulting distribution and its cumulative density function.

C Experiments

C.1 Sentiment Classification

For the sentiment classification experiment we downloaded¹² a pre-trained model from the Huggingface implementation¹³ of Wolf et al. (2019), and we fine-tuned on the SST dataset. We report hyperparameters used for training the model and our DIFFMASK in Table 3.

C.2 Question Answering

For the question answering experiment we downloaded¹² an already fine-tuned model from the Hug-

¹²https://huggingface.co/transformers/pretrained_models.html

Model	Value
Type	BERT _{LARGE} (uncased)
Layers	24
Hidden units	1024
Pre-trained masking	whole-word
Optimizer	Adam *
Learning rate	$3 \cdot 10^{-5}$
Train epochs	2
Batch size	24
DIFFMASK	Value
Optimizer	Lookahead RMSprop **
Learning rate ϕ, t	$3 \cdot 10^{-4}$
Learning rate α	$1 \cdot 10^{-1}$
Train epochs	2
Batch size	24
Constrain	$D_{\text{KL}}[y \hat{y}] < 2$

Table 4: List of hyperparameters for the question answering experiment. *is Kingma and Ba (2015), **is Tieleman and Hinton (2012); Zhang et al. (2019).

gingface implementation¹³ of Wolf et al. (2019) We report hyperparameters used by them for training the original model and the ones used for our DIFF-MASK in Table 4.

D Additional plots

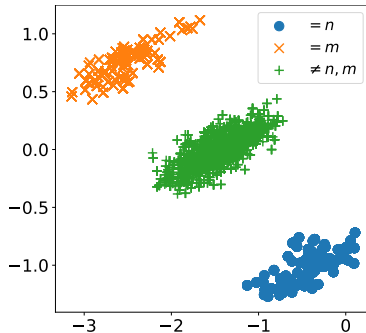


Figure 12: Hidden state values for the two-neuron toy task. Clusters of whether the input digit is equal to the first or second position in the query ($= n$ or $= m$ respectively) or not at all ($\neq n, m$) are completely linear separable.

¹³<https://github.com/huggingface/transformers>

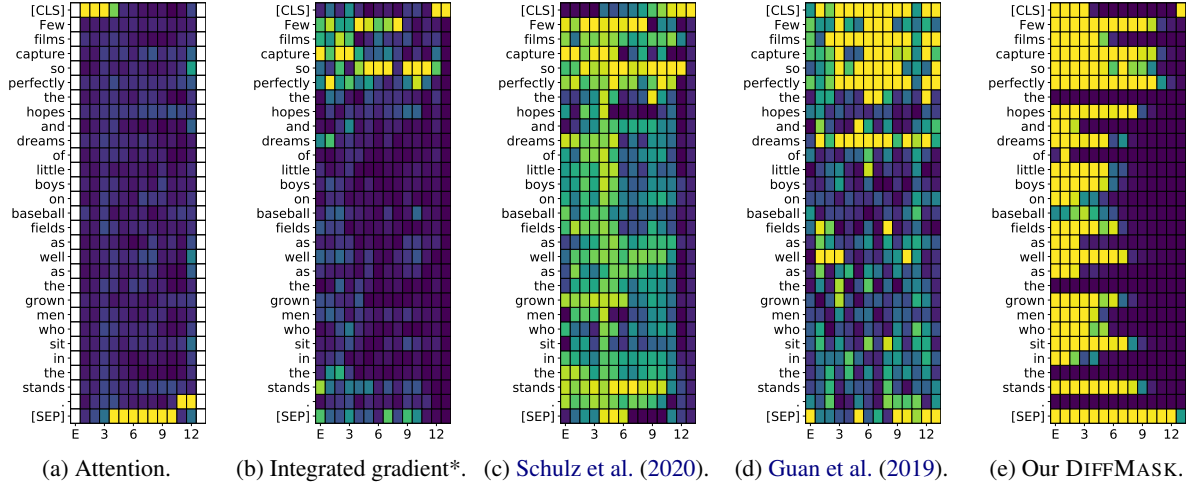


Figure 13: Sentiment classification: comparison between attribution method for hidden layers w.r.t. the predicted label. All plots are normalized per-layer by the largest attribution. Attention heatmap is obtained max pooling over heads and averaging across positions. *By Sundararajan et al. (2017).

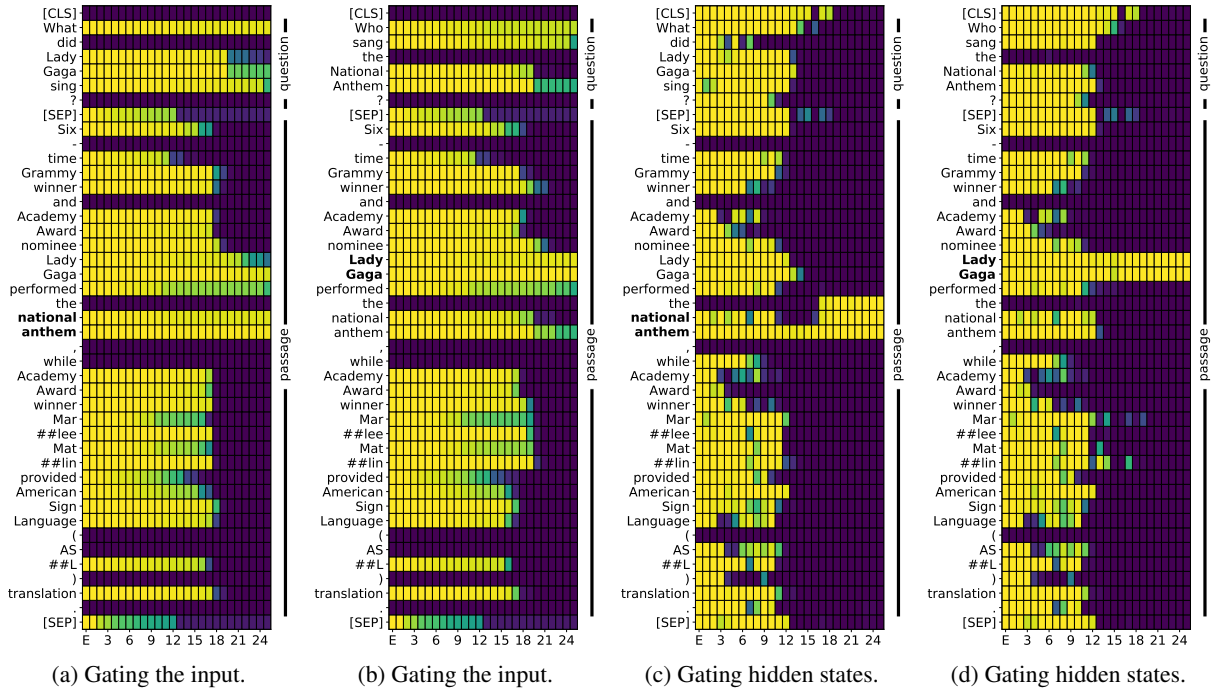


Figure 14: Expectation predicted by DIFFMASK to keep the inputs or hidden states on two different questions on the same paragraph. The correct answers is highlighted in bold.